ChemComm

ROYAL SOCIETY OF CHEMISTRY

FEATURE ARTICLE

View Article Online
View Journal

Cite this: DOI: 10.1039/d5cc06703k

Recent progress in NiFe-based catalysts for the high current density oxygen evolution reaction

Jaira Neibel Y. Bamba,[a] Maricor F. Divinagracia-Luzadas,[a] Donghyun Yoon,[bc] Jung-goo Choi,[bc] Joey D. Ocon*[d] and Jaeyoung Lee*[bce]

Received 25th November 2025,
Accepted 16th January 2026

DOI: 10.1039/d5cc06703k

rsc.li/chemcomm

The global transition to green hydrogen *via* water electrolysis is constrained by the sluggish oxygen evolution reaction (OER), particularly at high current densities required for industrial applications. Among Earth-abundant materials, nickel–iron (NiFe)-based compounds have emerged as leading candidates, offering intrinsic activity, synergistic interactions, and cost advantages that reduce the OER energy barrier, positioning them as viable alternatives to noble-metal catalysts such as IrO_2 and RuO_2. Yet, achieving long-term activity and structural stability at high current densities (HCDs) remains a critical challenge. This review highlights strategies to advance NiFe-based OER catalysts for sustained high-current operation, focusing on recent innovations including heteroatom doping, vacancy engineering, heterostructure formation, active-site modulation, and self-healing mechanisms. Developments across oxides, (oxy)hydroxides, non-metallic heteroatomic composites, layered double hydroxides, metal–organic framework-derived materials, and noble-metal-integrated hybrids are examined to provide a rational design framework for robust and efficient OER catalysts. Key pathways to tune morphology, composition, and electronic structure are identified, offering insights to bridge the gap between laboratory-scale studies and scalable electrolyzer deployment.

[a] Laboratory of Electrochemical Engineering (LEE), Department of Chemical Engineering, University of the Philippines Diliman, Quezon City, 1101, Philippines
[b] Ertl Center for Electrochemistry and Catalysis, Gwangju Institute of Science and Technology (GIST), 123 Cheomdangwagi-Ro, Buk-gu, Gwangju, 61005, South Korea
[c] Department of Environment and Energy Engineering, GIST, 123 Cheomdangwagiro, Buk-gu, Gwangju, 61005, South Korea
[d] Chemical Engineering Department, De La Salle University, 2401 Taft Avenue, Manila, 0922, Philippines
[e] International Future Research Center of Chemical Energy Storage and Conversion Processes (ifRC-CHESS), GIST, Gwangju, 61005, Republic of Korea

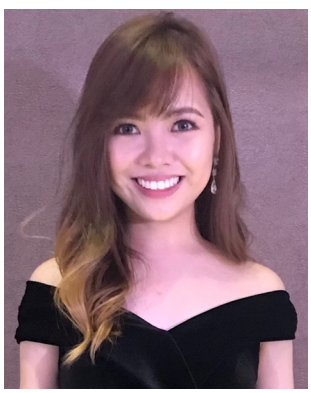

Jaira Neibel Y. Bamba

Jaira Neibel Y. Bamba received her bachelor's degree in chemical engineering in 2016 and her master's degree in chemical engineering in 2021 from Mapúa University. She later joined the Laboratory of Electrochemical Engineering (LEE) under the supervision of Prof. Joey Ocon to pursue her PhD in Chemical Engineering at the University of the Philippines Diliman. Her doctoral research centers on the development of advanced electrocatalysts for water splitting applications, aiming to enhance efficiency and durability in sustainable hydrogen production technologies.

Maricor F. Divinagracia-Luzadas

Dr Maricor F. Divinagracia-Luzadas received her PhD in Energy Engineering (2022) from the University of the Philippines Diliman, where she also received her BSc in Materials Engineering (2012) and MSc in Energy Engineering (2016). She now leads innovation in battery technology as the Electrochemistry R&D Division Head at Nascent Technologies Corp. Her research focuses on oxygen reduction (ORR) and oxygen evolution (OER) catalysts, battery energy storage systems, and next-generation lithium and post-lithium batteries, driving advancements in clean energy solutions.

1. Introduction

As the world shifts towards sustainable energy sources, hydrogen has emerged as a promising candidate for clean fuel due to its high energy density and zero-carbon emissions. A pivotal process for hydrogen production is water electrolysis, which splits water into oxygen and hydrogen. However, the efficiency of water electrolysis is limited by the sluggish oxygen evolution reaction (OER), a half-reaction involving a complex multielectron transfer process. Therefore, developing efficient, stable, and cost-effective OER catalysts is crucial for advancing hydrogen technologies.[1] Noble metal-based catalysts (Ru, Ir, and their oxides) are known for their superior OER activity but are constrained by their high cost and limited availability.[2] Consequently, there is a significant research interest in alternative catalysts composed of Earth-abundant materials. Among these, nickel- and iron-based compounds have garnered attention due to their inherent catalytic properties, affordability, tuneable properties, and synergistic

Donghyun Yoon

Donghyun Yoon received his MS degree from the School of Earth Sciences and Environmental Engineering at the Gwangju Institute of Science and Technology (GIST), South Korea, in 2023. He is currently pursuing his PhD in the Department of Environment and Energy Engineering at GIST. His current research focuses on developing in situ Differential Electrochemical Mass Spectrometry (DEMS) systems to analyze real-time products of various electrochemical reactions such as the OER, HER, and CO_2RR. He is also focusing on catalyst design for electrochemical CO_2 conversion to multi-carbon products, with an emphasis on investigating reaction intermediates and onset potentials.

Jung-goo Choi

Jung-goo Choi received his MS degree in the Department of Environment and Energy Engineering from GIST, South Korea. He is currently a PhD candidate in the same department. His current research interests are primarily focused on machine learning and electrochemistry. He has published scientific papers regarding electrochemical catalysts, single-cell systems, and electrochemical cell analysis utilizing machine learning in various international journals.

Joey D. Ocon

Prof. Joey D. Ocon is a Full Professor and Research Fellow at the Chemical Engineering Department of De La Salle University – Manila. He is a former Chair of the UP Diliman Department of Chemical Engineering, and he earned his BS (2008) and MS (2011) degrees in Chemical Engineering from the same university and his PhD in Environmental Science and Engineering (2015) from Gwangju Institute of Science and Technology, South Korea. He is a recognized national expert on batteries, fuel cells, electrochemical technologies, energy systems, and off-grid electrification and has led numerous R&D projects ranging from atomic-scale studies to energy systems research. He serves as an energy practice consultant for several organizations, including power companies, The World Bank and UNOPS-ETP. Prof. Ocon is also a co-founder and the President of the battery technology start-up Nascent Technologies Corporation and a Principal Strategist (Energy Transition) of the global sustainability organization Forum for the Future.

Jaeyoung Lee

Jaeyoung Lee is the vice director of the Ertl Center for Electrochemistry and Catalysis and a full professor at the Department of Environment and Energy Engineering, GIST, South Korea. He obtained his PhD under Prof. Gerhard Ertl (2001) from the Fritz-Haber-Institut der Max-Planck-Gesellschaft and FU Berlin, Germany. He was a senior scientist at RIST/POSCO (2002–2004) and at the Fuel Cell Research Center, KIST (2004–2007). His current research interests include Scale-up Science of water electrolysis, the CO_2RR, fuel cells and Li–S batteries. He is currently the academy director of ADeKo, the president of Humboldt Club Korea and the representative of MPG Korea Alumni.

effects that enhance OER activity.[3,4] However, commercial viability demands not only high activity but also long-term stability at high current densities ($\geq$200 mA cm^{-2}).[5,6] High-current-density (HCD) OER poses significant challenges due to the rapid formation of oxygen bubbles, which create concentration gradients, block active sites, and strain porous nanostructures.[7] At the same time, harsh oxidative conditions accelerate corrosion, leaching, and structural degradation of the catalyst. Surface reconstruction can sometimes be beneficial, exposing new active sites, but uncontrolled changes often lead to a decline in performance.[8,9]

Despite extensive efforts to enhance OER activity and elucidate the active sites of NiFe-based catalysts, relatively few studies have focused on achieving sustained high current densities ($\geq$200 mA cm^{-2}), which are equally vital for practical applications, and several critical gaps remain in the existing literature. Most existing studies and reviews primarily benchmark catalyst performance at low current densities (typically 10 mA cm^{-2}), often for limited durations and at room temperature, conditions that do not adequately reflect the harsh environments encountered in industrial electrolyzers.[10–12] Degradation mechanisms specific to high current regimes, particularly Fe leaching, surface reconstruction, and bubble-induced mechanical stress, remain insufficiently addressed, despite their critical impact on catalyst durability. Although Ni species are largely insoluble in alkaline media, Fe components are susceptible to leaching or segregation, potentially leading to uneven distribution of Fe elements or unwanted doping into the host lattice.[13] In addition, most prior reviews predominantly emphasize half-cell OER measurements, with comparatively limited discussion of overall water splitting and full electrolyzer performance. These factors accentuate the need for continuous improvement and development of durable NiFe-based catalysts through advanced strategies, including introducing vacancies to optimize the electronic structure, constructing heterostructures, enhancing interfacial interactions, doping with heteroatoms, *etc.*[13–17]

Considering these factors, this work provides an overview of recent design strategies for NiFe-based catalysts that exhibit high activity, stability, and current density, as illustrated in Fig. 1. Moreover, the advancements across various systems, including oxides, (oxy)hydroxides, non-metallic heteroatomic composites, layered double hydroxides (LDHs), metal–organic frameworks (MOFs), and noble metal-doped materials, have

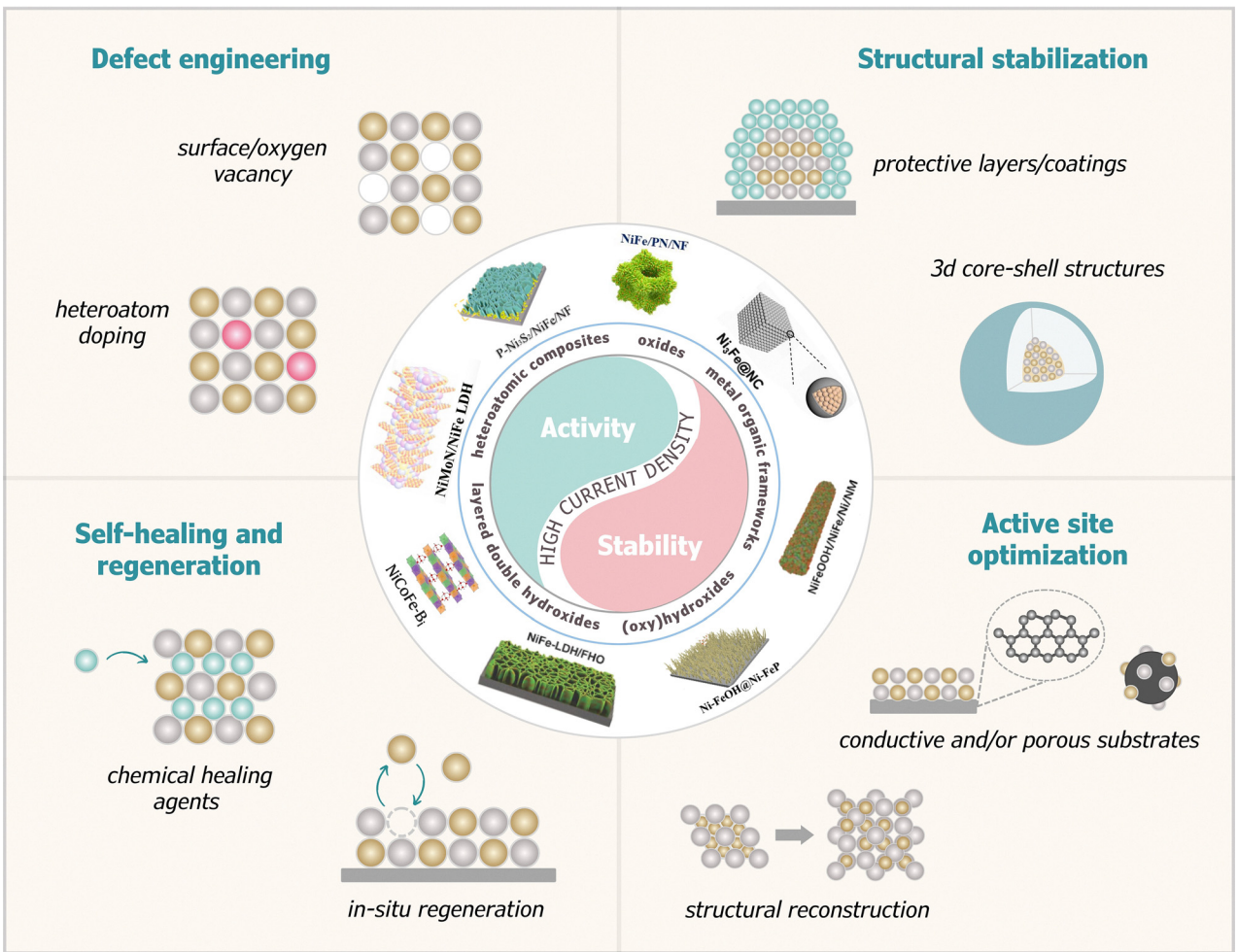

Fig. 1 Overview of recent design strategies for NiFe-based catalysts aimed at enhancing OER activity and stability at high current density (HCD).

been highlighted. Through a systematic examination of recent NiFe-based catalysts, this review elucidates the key factors governing HCD performance, specifically the necessity of balancing the adsorbate evolution mechanism (AEM) and the lattice oxygen mechanism (LOM) pathways, and the role of electronic structure modulation in stabilizing active species.

2. The OER mechanism of NiFe-based catalysts

The OER under alkaline conditions constitutes a complex multi-electron transfer process with O–O bond formation, rendering it more thermodynamically challenging compared to the two-electron hydrogen evolution reaction (HER). Thus, considerable efforts have been dedicated to deciphering the OER mechanism through kinetic studies, density functional theory (DFT) calculations, and operando or *in situ* spectroscopic techniques.[18–21] DFT is widely used to calculate the Gibbs free energy barriers ($\Delta G^{\ddagger}$) for reaction intermediates and identify the rate-determining step (RDS), offering theoretical insight into the preferred reaction channels. Operando and *in situ* spectroscopic methods (like Raman or X-ray absorption spectroscopy) are critical for observing dynamic changes in the catalyst structure and electronic environment during the OER, which helps validate computational models and track the formation of active species.[22]

OER mechanisms are typically classified based on the source of oxygen in O–O coupling: the adsorbate evolution mechanism (AEM), where oxygen originates from water molecules adsorbed onto the catalyst surface with metal ions as active sites, and the lattice oxygen mechanism (LOM), where oxygen comes from lattice oxygen ions within the catalyst structure, which themselves serve as active sites.[23] In the AEM, the reaction proceeds *via* sequential proton–electron transfer steps involving intermediates such as *OH, *O, and *OOH, with the metal cations facilitating adsorption and O–O bond formation. The activity of AEM catalysts is often limited by the intrinsic linear scaling relationship between *OH and *OOH adsorption energies, which imposes a theoretical overpotential threshold.[24] In contrast, the LOM involves direct participation of lattice oxygen in O–O coupling, generating transient oxygen vacancies that are replenished by water molecules from the electrolyte.[25] This pathway can bypass the scaling constraints of the AEM, potentially lowering the energy barrier for the OER, but may introduce structural instability if vacancy regeneration is insufficient. Recent DFT studies on the (001) facet of a nickel ferrite ($NiFe_2O_4$) catalyst revealed that the Fe-assisted LOM pathway is the preferred mechanism, exhibiting the lowest energy barrier ($\Delta G^{\ddagger}$ = 0.84 eV at U = 1.63 V_{SHE}) for the RDS involving O–O bond formation.[2] Another study proposed an AEM pathway (Fig. 2) for NiFe-based LDH catalysts at different electrolyte pH levels using combined electrochemical and operando spectroscopic measurements.[26] In alkaline media (pH ≥ 13), it was found that the adsorption of *OH occurs during the transformation from $Ni(OH)_2$ to NiOOH. The adsorption coverage of OH* is high during the OER, making this step both fast and efficient. Furthermore, a portion of *OH is converted to *O concurrently with the formation of Fe^{4+}, representing the pre-equilibrium step. The RDS involves the nucleophilic attack of OH^- on *O (Fe^{4+}=O) to generate M–OOH intermediates (M = Ni or Fe), with the final step being the rapid oxidation of *OOH and the release of O_2.

LOM-type mechanisms can enhance OER activity; however, catalysts typically undergo significant surface reconstruction during the LOM process due to the redox and migration of lattice oxygen, leading to potential catalyst dissolution and instability.[27] Conversely, catalysts generally exhibit higher stability but lower activity when following the AEM process.[28] Achieving sustained HCDs in NiFe-based materials critically relies on controlling the OER pathway between the high-activity, low-stability LOM and the high-stability, low-activity AEM. Specifically, advanced material engineering can be employed to tailor

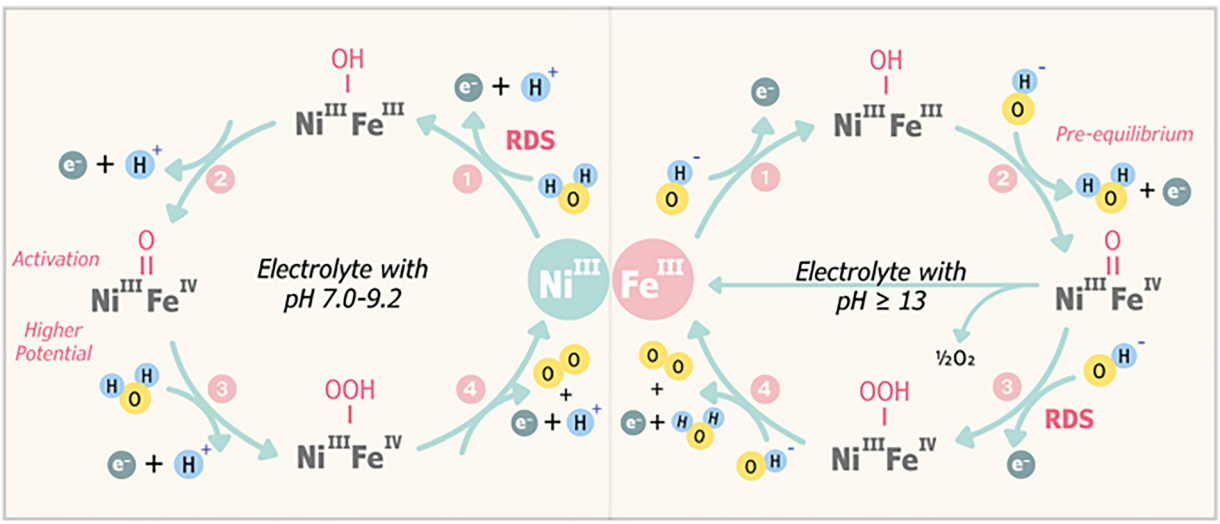

Fig. 2 Proposed reaction mechanism of oxygen evolution on NiFe-based LDH catalysts.

the catalyst's unique electronic structure, optimizing the adsorption of intermediates and effectively striking a balance between the LOM and the AEM to ensure optimal durability and performance.

3. Emerging NiFe-based materials for the high current density OER

Recent advancements have highlighted the potential of NiFe-based systems in achieving HCD with long-term stability for the OER. The synergistic interplay between Ni and Fe active sites within diverse structural frameworks, including oxides, (oxy)-hydroxides, non-metallic heteroatomic composites, LDHs, MOF-derived materials, and noble metal-doped compounds, is believed to underpin this exceptional performance. While existing review papers have comprehensively covered NiFe-based electrocatalysts for the alkaline OER,[29–31] a systematic analysis of catalysts capable of efficiently delivering HCDs remains limited. The succeeding sections address this gap by outlining robust NiFe-based materials reported over the last three years, prioritizing those demonstrating sustained HCD performance and detailing the synergistic design strategies that maximize stability and activity in commercially relevant environments.

3.1. NiFe-based oxides

Studies have consistently demonstrated that NiFe-based oxides exhibit superior activity compared to oxides based solely on Ni or Fe, attributed to a synergistic interplay between Ni and Fe.[32] Specifically, Ni lattices provide an ideal framework for anchoring Fe sites due to their exceptional electrical conductivity under anodic potentials.[33] Ni thus serves as a conductive scaffold, while Fe incorporation induces structural transformations, creating additional active sites and leading to an enhanced OER at HCDs. A recent theoretical investigation by Friebel *et al.*[34] explored the impact of bond lengths and Löwdin charges by varying Ni : Fe atomic ratios. The study found that Fe substitutes for Ni within the NiO_2 structure, forming Ni–O–Fe motifs that minimize overpotential (η) for the OER. Furthermore, a minimum Fe content of 10% has been identified as crucial for significant OER improvements in NiFe-based oxide catalysts.[35] Introducing oxygen vacancies (V_O) through dual-defect engineering can also enhance the electrical conductivity and intrinsic activity of NiFe-based oxides, leading to low overpotentials and good durability. Recently, Khatun *et al.*[36] developed a surface-modified Cr-doped $FeNi_3/NiFe_2O_4$ heterojunction OER catalyst rich in V_O. The generated V_O is believed to modulate the electronic configurations, creating numerous unsaturated coordinated metal active sites (Fig. 3a). This enhances the adsorption ability of oxygen intermediates, resulting in robust OER performance (η_{500} = 360 mV) and achieving sustainable HCD (200 h at 1000 mA cm^{-2}). It is also noteworthy that during the OER with NiFe-based oxides, intrinsic V_O can induce spontaneous electrochemical surface reconstruction, generating highly reactive (oxy)hydroxide (M–OOH) species, which are also recognized as active OER sites.[37]

NiFe-based oxides exhibit superior OER performance due to synergistic Ni–Fe interactions, where Ni provides a conductive framework and Fe creates highly active sites that lower overpotential, particularly at HCDs. Optimal Fe incorporation and oxygen vacancy engineering further enhance activity and durability by tuning the electronic structure, promoting active Ni–O–Fe motifs, and enabling dynamic surface reconstruction into catalytically active (oxy)hydroxide species.

3.2. NiFe-based (oxy)hydroxides

Early research on NiFe (oxy)hydroxide catalysts predominantly focused on powder forms. To enhance their performance, researchers have previously explored various strategies, including optimizing composition,[38] incorporating conductive carbon-based supports,[39] introducing structural/lattice defects,[40] *etc.* However, the inherent limitations of powder-based catalysts, such as durability and mass transport challenges, have hindered their practical applications in demanding environments like HCD electrolysis.[41] Due to these challenges, research has shifted towards developing alternative catalyst architectures. One promising approach involves the direct growth of catalysts on a conductive porous substrate/support. For instance, a recent study by Wu *et al.*[42] demonstrated the formation of NiFeOOH on a NiFe/Ni film through anodic electro-oxidation. The NiFe/Ni film, fabricated *via* a dynamic hydrogen bubble-templated process, facilitated efficient electron transport due to its high conductivity and served as a robust support for the catalyst layer. Additionally, the three-dimensional laminar porous structure of the film enhanced mass transport, reduced interfacial resistance, and maximized exposure of active sites. These combined factors contributed to the catalyst's enhanced performance (η_{1000} = 300 mV), enduring 100 h of testing at 500 mA cm^{-2}.

Interestingly, while Fe leaching is often considered detrimental to the stability of NiFe-based catalysts, recent studies have revealed its potential to enhance catalytic performance. Zhang *et al.*[43] showed that the partial dissolution/leaching of surface Fe atoms in a FeNi alloy exposes Ni sites (Fig. 3b), promoting lattice oxygen formation, which subsequently transforms into (oxy)hydroxides with low overpotential (η_{100} = 287 mV). Specifically, it activates the initially inactive Ni component, inducing the surface reconstruction of a FeNi–(oxy)-hydroxide/alloy heterojunction with longer N–O bonds within the (oxy)hydroxide structure compared to pure NiOOH. This significantly lowered the energy barrier for *OOH intermediate decomposition (Fig. 3c), enabling stable operation at HCD (80 h at 250 mA cm^{-2}). Meanwhile, Kang *et al.*[44] recently demonstrated that surface functionalization of NiFe (oxy)hydroxide catalysts (FSN) with tetraphenylporphyrin (TPP) significantly enhances their durability. O-labelling experiments combined with *in situ* Raman spectroscopy revealed that TPP does not alter the OER pathway of FSN, indicating that TPP's stability enhancement mechanism is unrelated to a shift from the LOM to the AEM. Instead, TPP functions as a protective layer, inhibiting the protonation of Fe–O sites and consequently reducing Fe dissolution. This protective effect enabled the TPP–FSN to maintain HCD (110 h at 500 mA cm^{-2}).

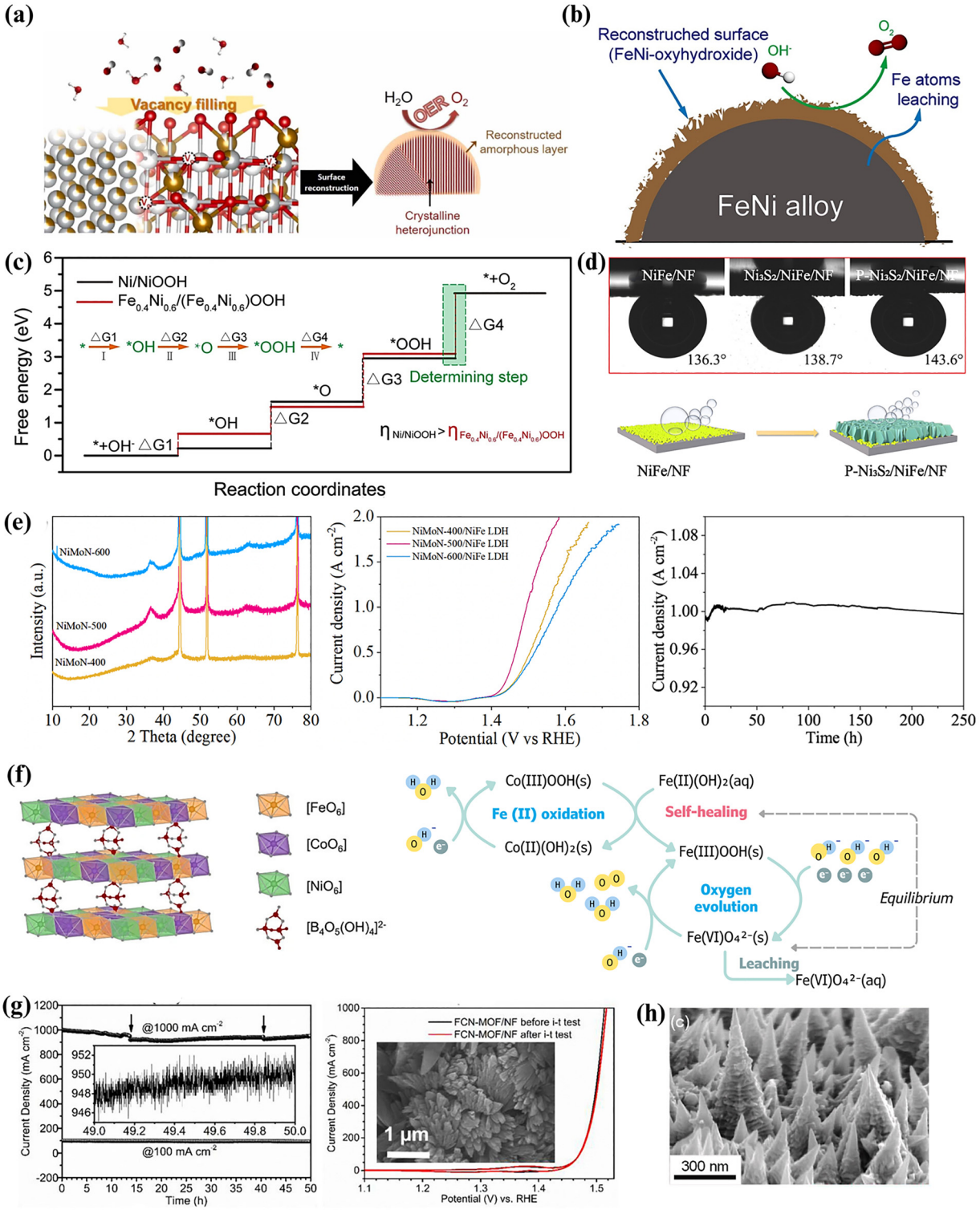

Fig. 3 (a) Schematic illustration of vacancy filling in Cr-doped $FeNi_3/NiFe_2O_4$ Mott–Schottky heterojunctions, accompanied by surface reconstruction that enhances OER performance. Reproduced from ref. 36. Copyright 2024, Elsevier. (b) Schematic illustration of partial Fe leaching and surface reconstruction in Fe_xNi_{1-x} alloy fiber paper. Reproduced from ref. 43. Copyright 2021, Elsevier. (c) Gibbs free energy diagram illustrating the four OER steps on $Fe_{0.4}Ni_{0.6}$ and $Fe_0Ni_{1.0}$ alloy fiber papers. Reproduced from Ref. 43. Copyright 2021, Elsevier. (d) Underwater aerophobicity of NiFe/NF, Ni_3S_2/NiFe/NF, and P–Ni_3S_2/NiFe/NF electrodes (top), and a schematic of their O_2 bubble adhesion behaviour (bottom). Reproduced from ref. 46. Copyright 2022, Elsevier. (e) XRD pattern of NiMoN–T and OER polarization curve of NiMoN–T/NiFe LDH (T represents the nitridation temperature). Chronoamperometry curve of NiMoN/NiFe LDH for 250 h. Reproduced from Ref. 54. Copyright 2023, Springer Nature. (f) Schematic illustration of the structure of NiCoFe–B_i and its self-healing mechanism, catalysed by Co. Reproduced from ref. 68. Copyright 2021, Springer Nature. (g) Chronoamperometric stability and cyclic voltammetry curves of FCN-MOF/NF at 1000 mA cm^{-2}. Reproduced from ref. 72. Copyright 2020, Elsevier. (h) Scanning electron microscopy (SEM) image of NiFe nanocones with a superhydrophilic surface, enabling rapid mass transfer in an industrial water electrolyzer. Reproduced from ref. 85. Copyright 2024, Elsevier.

Another effective strategy to enhance performance in these systems is to design three-dimensional nanostructured catalysts that enlarge the specific surface area, expose more active sites, and create heterojunctions between the metallic core and the (oxy)hydroxide shell to improve charge transport. For example, hierarchical $FeNi_3$@(Fe,Ni)S_2 core–shell heterojunctions with a tunable shell thickness were fabricated through $NiFe(OH)_x$ reduction followed by partial sulfidization.[45] The analysis revealed that the $FeNi_3$ core substantially increases the conductivity, acting as an electron highway, while the (Fe,Ni)S_2 shell provides an active surface for the *in situ* generation of S-doped NiFe (oxy)hydroxides with remarkable OER activity (η_{100} = 288 mV) and stability (1200 h at 200 mA cm^{-2}). Notably, S-doping was also found to improve the conductivity of the catalyst, as evidenced by the reduced bandgap of S–Ni_x-$Fe_{1-x}OOH$ compared to $Ni_xFe_{1-x}OOH$, contributing to the enhancement of catalytic performance.

NiFe-based (oxy)hydroxide catalysts have evolved from powder systems toward engineered architectures that address durability and mass-transport limitations at HCDs. Strategies such as direct growth on conductive porous substrates, controlled Fe leaching, surface protection to suppress Fe dissolution, and 3D core–shell or heterojunction designs collectively enhance conductivity, active-site exposure, and structural stability, enabling sustained OER operation under industrially relevant conditions.

3.3. Non-metallic heteroatomic combinations

To boost intrinsic activity and stability, pristine catalysts often require surface and/or structural modifications by introducing heteroatoms like P, S, N, and C to form stable functional groups. Oxidation states and electronic structures are modified, generating defects that aid HCD operation.

3.3.1. Phosphides. Since the water electrolysis reaction occurs at the three-phase gas–liquid–solid interface, the OER is influenced not just by the intrinsic activity but also by the surface properties of the tested working electrode and catalyst. Consequently, a distinctive aerophobic structure is crucial for an efficient OER under these conditions. The recent findings by Zhang and co-workers[46] demonstrate that synergistically incorporating P and S ions into $NiFeO_x$ electrocatalysts (NiFe/NF) can modify their interfacial and surface characteristics, leading to optimized surface properties. The resulting P–Ni_3S_2/NiFe/NF catalyst exhibited a lower surface contact angle compared to NiFe/NF and Ni_3S_2/NiFe/NF, indicating enhanced aerophobicity, as shown in Fig. 3d. Similarly, recent studies in HCD electrolysis have demonstrated that ordered porous structures and steric confinement effects can modulate local reactant–surface interactions and mass transport, emphasizing the importance of optimizing triple-phase interfaces.[47,48] These insights provide valuable conceptual guidance for enhancing HCD OER performance by improving gas transport, bubble detachment, and interface stability.

Meanwhile, integrating P into the S structure induces electron transfer from Ni to S *via* heterointerface formation, creating favourable hydride-acceptor ($Ni^{\delta+}$) and proton-acceptor ($S^{\delta-}$–$P^{\delta-}$) sites. This optimized electronic configuration, coupled with improved aerophobicity, enables the catalyst to achieve exceptional activity (η_{1000} = 372 mV) and stability at HCD (20 h at 1000 mA cm^{-2}). Additionally, the –PO_4 groups contribute by lowering the free-energy barrier for the OER at NiFe sites. Other works have also shown that phosphate ions in LDHs improve mass transfer and catalyst durability by mitigating metal leaching caused by local OH^- depletion.[49] Similarly, Sheng *et al.*[50] observed improved overall durability in a NiFe–P catalyst despite slight structural instability. The catalyst films, synthesized *via* flame aerosol deposition, were initially encapsulated by a carbonaceous (soot-like) matrix. The controlled electrochemical removal of this carbon under OER conditions triggered a self-refreshing mechanism, causing gradual and mild detachment of the film material while continuously exposing fresh catalytic sites. This dynamic process mitigated the selective leaching of Fe, preserving an Fe-rich, highly active surface. As a result, high activity (η_{10} = 245 mV) and stability (100 h at 500 mA cm^{-2}) were achieved at HCD.

NiFe–P catalysts have spurred considerable research interest in recent years due to their bifunctional activity towards both the OER and the HER across various pH conditions. Recently, Hu *et al.*[51] developed a core–shell Ni–FeOH@Ni–FeP bifunctional catalyst for overall water splitting (OWS) and proposed a reaction mechanism in which FeOOH transiently forms at Fe sites with a low theoretical overpotential (0.14 eV). However, the subsequent O_2 release from FeOOH is hindered by a high overpotential (0.63 eV), whereas the transition from FeOOH to NiOOH occurs with a lower energy barrier ($\approx$0.43 eV), and O_2 release from NiOOH is more favourable (0.2 eV). The presence of Fe in the Ni–FeOH@Ni–FeP electrode facilitates NiOOH formation, thereby enhancing OER activity. Additionally, the hydroxide layer interacts with the phosphide core, modulating electronic structures and surface microenvironments. This interaction regulates FeOOH formation rather than completely suppressing it, ensuring a balance between active site regeneration and catalytic efficiency. Hence, the catalyst exhibited remarkable stability at HCDs of 750 and 935 mA cm^{-2} in OWS.

NiFe-based phosphide catalysts enhance the HCD OER by optimizing triple-phase interfaces through improved aerophobicity, porous architectures, and interfacial electronic modulation. Phosphorus incorporation and heterointerface formation promote efficient charge transfer, favorable intermediate energetics, suppressed metal leaching, and self-refreshing or stabilized active surfaces, enabling high activity and durability at industrially relevant current densities.

3.3.2. Sulphides. The incorporation of sulphides/sulphur vacancies (V_S) into catalyst structures has been shown to significantly boost NiFe performance by modifying the material's electronic properties, as demonstrated by the computational studies of He *et al.*[52] Under OER conditions, the thermodynamic preference for oxide formation makes sulphides susceptible to oxidation, leading to the potential formation of (oxy)sulphide intermediates. The oxidation of divalent metal ions to trivalent states within the S structure during the OER can generate fresh oxysulphide phases, exposing new active sites that enhance

catalytic activity (η_{1000} = 235 mV) and stability (260 h at 500 mA cm^{-2}). S-rich materials with abundant V_S tend to contain more divalent metallic elements, which are beneficial for the *in situ* generation of active oxysulphides after HCD OER tests, thereby maintaining V_S and ensuring high durability. Computational modelling further suggests that these V_S improve electrical conductivity, with Fe sites identified as primary active centers. Similarly, combined computational modelling and operando characterization revealed that optimal S contents in sulphur-tuned, low-crystalline-reduced NiFe-based coordination polymer catalysts (S–R–NiFe–CPs) can effectively regulate local electronic structures compared to S-free O_d–R–NiFe–CPs.[53] This promotes the generation of highly oxidized Fe^{4+} and Ni^{4+} species, leading to oxygen-bridged Ni^{IV}–O–Fe^{IV} moieties, which serve as the true OER active intermediates and enable the system to reach HCD operations.

Sulphide incorporation and sulphur vacancy engineering in NiFe catalysts enhance the HCD OER by tuning electronic structures, improving conductivity, and enabling *in situ* formation of active oxysulphide and high-valence Ni^{4+}/Fe^{4+} species. These dynamic transformations expose new active sites, stabilize sulphur vacancies, and promote oxygen-bridged Ni–O–Fe intermediates, resulting in high activity and durability under demanding electrolysis conditions.

3.3.3. Nitrides. Nitrogen's lone pair electrons promote stronger interactions with OER reactants, making N-doping an effective strategy to elevate the performance of NiFe-based materials under HCD conditions.[6] Zhai *et al.*[54] developed a hierarchical core–shell nitride/hydroxide catalyst (NiMoN/NiFe LDH) to regulate the electronic states of active sites and enhance OER activity. As shown in Fig. 3e, optimizing the nitridation temperature influenced the crystallinity and catalytic performance of NiMoN/NiFe LDH, with 500 °C identified as the best condition. The optimized catalyst outperformed $MoNi_4/MoO_2$/NiFe LDH and $NiMoO_4$/NiFe LDH, achieving a stable OER at HCD (250 h at 1000 mA cm^{-2}), attributed to enhanced conductivity and accelerated electron transport from nitridation treatment. Meanwhile, N-doping is known to alter the d-electron density of the metal, leading to a contraction of the d-band structure that resembles the electronic structure of noble metals near the Fermi level, potentially contributing to the enhanced stability at HCD.[55] However, though studies show that N-doping has potential for improving OER activity,[56,57] a critical gap exists in the literature regarding the long-term stability of these materials under HCD conditions, as most reports only cover stability testing at 10 mA cm^{-2} or below 200 mA cm^{-2}.

Nitride formation and N-doping enhance NiFe-based OER catalysts at HCDs by strengthening reactant interactions, tuning electronic structures, and improving conductivity and charge transport. Core–shell nitride or hydroxide architectures demonstrate exceptional HCD stability, although long-term durability data at industrially relevant current densities remain limited in the literature.

3.3.4. Carbides. Integrating inexpensive, chemically stable, and highly conductive carbon materials is another approach to boost OER performance by exposing more active sites and enhancing electron transport. Carbon supports can also improve the stability of NiFe catalysts under demanding operating conditions. A notable example is Li *et al.*'s[58] self-supported tellurium (Te)-doped $NiFe_2O_4$ with a carbon-stabilized nanosheet structure on nickel foam (Te–$NiFe_2O_4$@C/NF), fabricated *via* NiFe LDH calcination. Experimental and DFT studies confirmed that the low overpotential (η_{500} = 180 mV) and remarkable stability of the catalyst can be attributed to the highly graphitized carbon layer, which exhibits strong oxidation resistance, effectively protecting the active sites of the Te–$NiFe_2O_4$@C/NF nanoparticles. It was also found that Te-doping altered the local electron environment, adjusting the interaction intensity between the adsorption intermediate and the active site, thus lowering the energy barrier for the OER step. Impressively, the catalyst had negligible degradation after a 180-h stability test at 500 mA cm^{-2}. In another report by Wang *et al.*,[59] encapsulating $Fe_{0.5}Ni_{0.5}$ alloy nanoparticles within a porous carbon matrix can both enhance the OER (η_{10} = 219 mV) and effectively prevent agglomeration, which is a common challenge for nanosized particles that can impair catalytic activity, thereby eliminating the need for surfactants. Despite these advances, the durability of most of these catalysts at HCD is still unclear, warranting further investigations.

Carbon integration in NiFe-based catalysts enhances OER performance by improving electrical conductivity, exposing active sites, and stabilizing catalysts under harsh conditions. Graphitized or porous carbon structures, coupled with dopants or alloy encapsulation, protect active phases, suppress agglomeration, and lower OER energy barriers.

3.4. NiFe-based layered double hydroxides

For LDHs or other NiFe-based materials in general, the synergistic effect among multiple metal ions is not limited to Ni and Fe. Adding a third metal may further improve the catalytic performance by effectively changing the adsorption/desorption energy and surface electronic structure of LDH catalysts.[60] Wu *et al.*[61] employed a ternary NiFeCo LDH through operando incorporation of Co^{2+} into the NiFe LDH catalyst (NiFeCo-0.6), identifying 0.6 mmol as the optimal Co-doping content. Here, Co-doping reduced the Ni oxidation potential and accelerated the formation of highly active $Ni(Co)_{1-x}Fe_xOOH$ species during the OER, resulting in lower overpotential (η_{1000} = 353 mV) compared to pristine NiFe LDH (η_{1000} = 502 mV). Co-doping also enabled NiFeCo-0.6 to follow the LOM pathway with a lower RDS Gibbs free energy (0.35 eV) than that of NiFeOOH (1.23 eV). Additionally, the Fe dissolution rate in NiFeCo-0.6 was lower than that of NiFe LDH, indicating greater stability. It showed that Co-doping stabilized the Fe local coordination environment, reducing dissolution and enhancing the overall stability of the NiFeCo-0.6 catalyst (300 h at 500 mA cm^{-2}). Similarly, various metals have also been used to improve the performance of NiFe-based LDHs.[62–64] To fully optimize trimetallic LDH systems, a comprehensive understanding of the interplay between metal ion species within the brucite layers and the nature of the interlayer anions is crucial, as these factors collectively influence activity and stability.

Defect modification can also be an efficient and cost-effective way to achieve high-performance NiFe LDHs. According to the DFT study of Mohammed-Ibrahim,[65] creating unsaturated NiFe coordination sites in LDHs through defect engineering of Ni–O–Fe coupling at the atomic scale can reduce the Gibbs free energy of the deprotonation step in the OER. In another study by Wang *et al.*,[66] a hexagonal NiFe–LDH/FeOOH heterostructure with oxygen defects was synthesized using a facile hydrothermal method, based on the *in situ* competing growth strategy of bimetallic ions and OH^- ions. Oxygen defects were found to enhance OH^- nucleophilic attack and promote synergy at Fe–O sites, particularly between the AEM and the LOM, thereby maximizing the utilization of surface metals and oxygen atoms. The projected density of state (PDOS) analysis showed that introducing V_O shifts the Fe-3d band center down, reducing over-strong adsorption and weakening the Fe–O bond, thus enhancing both AEM and LOM catalytic performance. As a result, the catalyst exhibited low overpotential (η_{1000} = 353 mV) and remarkable stability (20 h at 1000 mA cm^{-2}) at HCDs.

Another emerging strategy to mitigate the instability of NiFe-based LDH materials involves investigating their capacity for self-repair or regeneration. Recent studies have demonstrated the potential of such systems to restore catalytic activity and maintain stability at HCDs.[67–69] For instance, the presence of both ferrous and borate ions in the electrolyte was critical for the self-healing of a borate-intercalated NiCoFe–LDH (NiCoFe–B_i).[68] The addition of ferrous ions restored Fe content by activating a self-healing mechanism (Fig. 3f) where Co catalyses the redeposition of Fe oxyhydroxide, compensating for the leaching of Fe active sites. Concurrently, borate ions prevented further degradation by replenishing the depleted borate ions within the LDH structure, resulting in sustained stability (100 h at 500 mA cm^{-2}). However, the exploration of the self-healing ability of NiFe-based materials remains relatively untapped and requires further investigation, as their effectiveness is contingent on factors including catalyst properties, electrolyte and buffer composition, pH, applied current and potential, temperature, and mass transport conditions.

NiFe-based LDH performance at HCDs can be significantly enhanced through multimetal synergy, defect engineering, and emerging self-healing strategies. Trimetallic doping (*e.g.*, Co) tunes the electronic structure, lowers overpotential, suppresses Fe dissolution, and stabilizes active oxyhydroxide species, while oxygen vacancies optimize adsorption energetics and promote dual AEM/LOM pathways; additionally, electrolyte-assisted self-repair mechanisms offer a promising route to sustain long-term stability under harsh OER conditions.

3.5. MOF-derived NiFe-based catalysts

NiFe-based MOFs often suffer from leaching/exfoliation under testing conditions, significantly impacting long-term stability.[70] To address this, the interaction between catalysts and support should be reinforced, as the adhesion between them may be insufficient to withstand the stresses induced by gas bubble formation during HCD operations.[71] One of the effective strategies to tackle this issue is the *in situ* growth of catalysts on conductive 3D porous substrates. For example, equimolar Fe-, Co-, and Ni(FCN)-based trimetallic MOFs, grown *in situ* on NF, exhibited exceptional OER activity (η_{1000} = 284 mV), operating at a HCD of 1000 mA cm^{-2} with only a 5% decay after 50 h (Fig. 3g).[72] The binder-free, *in situ* growth strategy enhanced both mechanical adhesion and intrinsic activity by promoting synergistic interactions among the well-dispersed metal ions within the MOF structure. The intrinsically low electrical conductivity and mass permeability of many NiFe-based MOFs limit their direct use as catalysts. Instead, these materials are often used as precursors to derive composites containing NiFe derivatives as active species through high-temperature thermal treatments. The incorporation of good conductors, such as carbon nanotubes (CNTs) and graphene, has also been explored to improve OER performance, as their higher degree of graphitization provides better structural stability and resistance to carbon corrosion induced by oxidation currents. A recent study by Wang *et al.*[73] demonstrated the effectiveness of anchoring FeNi LDH nanoflakes onto MOF-derived CNT networks to create stable, self-supported catalysts, achieving low overpotential (η_{10} = 200 mV) and robust stability for over 160 h at 1000 mA cm^{-2}. Meanwhile, the scalability and cost-effectiveness of MOF-derived NiFe catalysts pose challenges for practical applications. Most of their metal oxides are produced *via* calcination with low yields.[74] Thus, exploring new synthesis strategies to improve product yield and preparation efficiency is both important and urgent.

MOF-derived NiFe catalysts address the instability and poor conductivity of pristine MOFs by strengthening catalyst–support interactions and enhancing charge transport. Strategies such as *in situ* growth on conductive 3D substrates and conversion into carbon- or CNT-integrated NiFe derivatives improve mechanical adhesion, activity, and durability at HCDs, although scalability and low-yield synthesis remain key challenges for practical deployment.

3.6. Noble metal-containing NiFe-based catalysts

In recent years, several groups have reported that integrating noble metals (NMs) into NiFe-based catalysts offers a promising avenue for enhancing activity and durability while mitigating the reliance on these scarce and costly resources.[75,76] While NM oxides like RuO_2 exhibit superior OER activity, their instability under harsh operating conditions remains a critical challenge.[77] To address these, researchers have explored strategies to maximize the utilization of NMs through size reduction and structural optimization.[76,78,79]

Single-atom catalysts (SACs) represent the ultimate limit in terms of particle size and offer the potential to overcome the cost and stability challenges associated with traditional NM-based catalysts.[80] Recent studies have demonstrated the feasibility of incorporating NM single atoms (SAs) into complex nanostructures to achieve exceptional OER performance.[81] For instance, Wang *et al.*[78] developed a bifunctional catalyst comprising Ru_{SAs} integrated into a $Ni(OH)_2$–FeOOH nanowire heterostructure with enhanced stability. The unique architecture

exhibited superior aerophobicity, facilitating efficient mass transport and bubble removal, which is a common cause of active layer degradation. The synergistic interplay among Ru_{SAs}, FeOOH clusters, and the porous nanostructure resulted in enhanced active site exposure (η_{1000} = 386 mV) and accelerated reaction kinetics, leading to a minimal overpotential increase after 140 h of stability testing at 500 mA cm^{-2}. In another aspect, the structural mismatch between LDHs can generate abundant defects, providing ideal supports and unique anchoring sites for NM atoms. Van *et al.*[75] demonstrated that the strong electronic interaction between lanthanum (La) and the host metals in a NiFe LDH not only considerably increased the number of catalytic sites and reduced charge transfer resistance but also elevated Fe d-band levels and created more V_O than in pristine NiFe catalysts, leading to superior activity (η_{500} = 309 mV) and long-term stability (600 h at 500 mA cm^{-2}). Similarly, Hu *et al.*[79] reported an Ir_{SAC}–NiFe–LDH catalyst with long-term stability (120 h at 200 mA cm^{-2}), where charge redistribution at the active Ni sites (induced by the high-valence Ir_{SAs}) lowered the energy barrier of *OOH dissociation *via* the AEM pathway, thereby facilitating the fast reaction kinetics of Ir_{SAC}–NiFe–LDH. Beyond serving as anchoring sites, the interaction between monatomic NM atoms and the NiFe-based support in determining activity/stability at HCDs is still elusive for SACs, which should be of critical importance for maximizing the efficiency of NMs and exploring novel properties.

Incorporating noble metals into NiFe-based catalysts, especially as single-atom sites, enhances OER activity and durability by improving active-site exposure, accelerating reaction kinetics, and facilitating mass transport. Strategies like size reduction, defect-rich supports, and heterostructure engineering maximize noble-metal utilization, while electronic interactions with the NiFe host further optimize activity and stability at HCDs, though the full mechanisms in single-atom systems remain underexplored.

As a summary, Table 1 lists the catalytic activity and HCD stability of recently reported NiFe-based catalysts designed for HCD operations. For the alkaline OER, strategies such as heteroatom doping, heterostructure formation, and defect/vacancy engineering have proven to be effective in modulating the physical, electronic, chemical, and surface properties of catalysts. These modifications directly influence intermediate adsorption/desorption, the OER mechanism, and charge transfer kinetics, leading to substantial enhancements in intrinsic activity. Additionally, employing techniques like *in situ* growth on conductive substrates, surface wettability engineering, and the creation of 3D porous architectures can significantly extend the catalyst lifespan and boost overall performance, aligning with the commercial requirements of practical water electrolysis.

Importantly, the performance descriptors governing NiFe-based electrocatalysts vary significantly across different electrochemical processes. In half-cell OER measurements, activity is primarily governed by intrinsic parameters such as the Fe coordination environment, electronic structure modulation,

Table 1 Stability of the reported NiFe-based OER catalysts at high current densities

Catalyst	Design strategy used	Overpotential	Stability test	Electrolyte	Remark after the stability test
NiFeOOH/NiFe/Ni[42 a]	Core–shell heterostructure	300 mV at 1000 mA cm^{-2}	100 h at 500 mA cm^{-2}	1 M KOH	Small voltage decrease
P–Ni_3S_2/NiFe/NF[46]	Phosphorous-doped (or phosphide) heterostructure	372 mV at 1000 mA cm^{-2}	20 h at 1000 mA cm^{-2}	1 M KOH	Pristine structure and morphology were retained
NiMoN/NiFe LDH[54]	Core–shell heterostructure/nitrogen doping	266 mV at 1000 mA cm^{-2}	250 h at 1000 mA cm^{-2}	1 M KOH	Negligible degradation
NiFe–P-1.88[50]	Phosphorous (or phosphide) doping	360 mV at 1000 mA cm^{-2}	100 h at 500 mA cm^{-2}	1 M KOH	Reasonable stability
CeF_3–NiFe LDH[91]	Heteroatom doping/surface modification	340 mV at 1000 mA cm^{-2}	90 h at 500 mA cm^{-2}	1 M KOH	No significant change
NiFe–S-0.6[52 a]	Sulphur (or sulphide) doping	235 mV at 1000 mA cm^{-2}	140 h at 500 mA cm^{-2}	6 M KOH	Only 8.9% increase in potential
NiFeCo-0.6[61]	Ternary LDH/co-doping/optimized LOM pathway	353 mV at 1000 mA cm^{-2}	300 h at 500 mA cm^{-2}	1 M KOH	Negligible degradation
$WO_2Ni_{17}W_3$/NiFe$(OH)_x$/NF[92 a]	Core–shell heterostructure/heteroatom doping	338 mV at 1000 mA cm^{-2}	120 h at 1000 mA cm^{-2}	6 M KOH	Negligible potential rise
Ni_3S_4/FeS (FNF-0.5 V)[93]	Sulphide-doped heterostructure	395 mV at 1000 mA cm^{-2}	200 h at 1500 mA cm^{-2}	1 M KOH	No significant degradation
MoS_2/$NiFeS_2$/NF[94]	Sulphide-doped heterostructure	314 mV at 1000 mA cm^{-2}	35 h at 500 mA cm^{-2}	1 M KOH	Only a 76 mV increase in potential
NiFe–LDH/FHO[95]	LDH heterostructure	248 mV at 500 mA cm^{-2}	1000 h at 500 mA cm^{-2}	1 M KOH	Only a 30 mV increase in potential
NiFeLa LDH-2[75 a]	Heteroatom doping/defect engineering	309 mV at 500 mA cm^{-2}	600 h at 500 mA cm^{-2}	1 M KOH	No significant degradation
Cr-doped (4 mol%) $FeNi_3$/$NiFe_2O_4$[36]	Oxide heterojunction/dual-defect engineering	360 mV at 500 mA cm^{-2}	200 h at 1000 mA cm^{-2}	1 M KOH	No noticeable decay
Fe,N–Ni$(OH)_2$/NF[6]	Nitrogen doping	340 mV at 500 mA cm^{-2}	10 h at 500 mA cm^{-2}	1 M KOH	Excellent potential sustention
NiFe/PN/NF[96 a]	Phosphorous/nitrogen-doped (dual-doping)	297 mV at 500 mA cm^{-2}	40 h at 500 mA cm^{-2}	6 M KOH	Only a 20 mV increase in potential

[a] Catalyst performance was tested in an alkaline electrolyzer or under simulated industrial conditions.

and adsorption energetics of oxygen intermediates.[37] However, under bifunctional operation or full-cell electrolysis, additional parameters, including catalyst–support adhesion, bubble management, mass transport, and structural robustness under continuous polarization, become equally critical.[82] For instance, strategies that promote surface reconstruction and lattice oxygen participation may enhance intrinsic OER kinetics in half-cell tests but can accelerate Fe dissolution and structural degradation during prolonged high-current operation in electrolyzers.[7] This process-dependent behavior highlights the necessity of tailoring NiFe catalyst design according to the targeted electrochemical configuration rather than relying solely on half-cell performance metrics.

4. Scale-up technologies

Shifting focus towards large-scale systems, the performance and durability of NiFe-based catalysts in a full electrolyzer cell may deviate from half-cell tests due to variations in pH, temperature, and pressure.

While HCDs can enhance reaction kinetics, they also entail higher investment costs, requiring a balance between cost and efficiency to optimize current density. Moreover, concentration polarization and severe localized stresses induced by rapid gas bubble generation in HCDs can compromise catalyst stability, ultimately leading to inactivity.[83,84] To ensure the longevity and efficiency of electrolyzers, it is essential to examine the catalyst performance within the context of the entire system's operations. Liu *et al.*[85] employed an alkaline electrolyzer using an optimized NiFe alloy anode and NiMo cathode, operating at 80 °C with a 30 wt% KOH electrolyte. The superhydrophilic structure of the NiFe catalyst (Fig. 3h) helped enhance mass transfer and likely minimized gas bubbles that could obstruct active sites during operation. This led to a low cell voltage (1.841 V at 500 mA cm^{-2}) and reduced energy consumption (4.4 kWh Nm^{-3} H_2). In addition to its high activity, the NiFe//NiMo electrolyzer demonstrated exceptional durability, maintaining stable operation at HCD (50 h at 500 mA cm^{-2}). Similarly, Ha *et al.*[86] developed a NiFeV-oxide thin-film electrocatalyst *via* magnetron sputtering, introducing oxygen vacancies that enhanced catalytic activity. Operando Raman spectroscopy revealed that these vacancies, along with vanadium leaching, promoted surface reconstruction into NiFe(oxy)hydroxide, optimizing water adsorption and accelerating the OER. The single-stack NFV-0.7(−)‖NFV-0.7(+) electrolyzer, operating at 60 °C, achieved a low cell voltage (1.84 V at 1000 mA cm^{-2}), attributed to the formation of V_O species resulting from vanadium substitution into NiFe, as well as robust stability at the same current density for 50 h, demonstrating its potential for industrial-scale electrolysis. In another study, Fe ions were introduced as electrolyte additives to promote the activity of NiFe LDH in an anion exchange membrane water electrolyzer, resulting in a low cell voltage of 1.73 V and a high energy conversion efficiency of 69.4% at 3000 mA cm^{-2}.[87] Additional comprehensive stability assessments under simulated industrial conditions have recently been carried out, offering more reliable quantitative data and enabling a more effective comparison of the scalability potential of NiFe-based catalysts.[88–90]

5. Conclusions and future perspectives

The development of NiFe-based catalysts for the oxygen evolution reaction (OER) has progressed rapidly, yet achieving simultaneous high activity and long-term stability at high current densities (HCDs) remains a critical challenge. Stability is as crucial as intrinsic catalytic performance, particularly under harsh oxidative conditions encountered in industrial water electrolysis. Protective coatings, such as carbon-based layers and metal oxides, can shield NiFe catalysts from corrosion and structural degradation, but their effectiveness depends on chemical robustness and electrical conductivity. Core–shell architectures, in which a stable shell encases a reactive NiFe core, can extend the operational lifespan by preserving the active core, yet the precise mechanisms that govern activity retention remain poorly understood. To fully understand the precise mechanism by which performance is enhanced in these systems, further in-depth investigations are still necessary. Future research must employ advanced operando and *in situ* characterization techniques to definitively resolve the precise OER mechanism in complex systems, such as core–shell structures. Crucially, the location of the true active site, whether it resides on the conductive core, the protective shell, or the reconstructed interface, remains a subject of debate that must be clarified to enable rational catalyst optimization.

High catalytic performance also requires large surface areas and dense active sites, ideally integrated on three-dimensional conductive porous substrates to enhance mass transport, electron conductivity, and bubble management. Gas bubble accumulation at HCDs can impede reaction kinetics and damage nanostructures. Strategies including surface (wettability) engineering, hierarchical porosity, superaerophobic or superhydrophilic interfaces, conductive scaffolds, and flow-assisted bubble removal can improve gas evacuation, stability, and overall performance. Structural reconstruction during the OER can either expose new active sites or degrade catalysts, and its beneficial aspects can be further optimized through defect engineering, alloying, heteroatom doping, and self-healing materials, enhancing durability under demanding conditions.

Despite these advances, key challenges remain. A comprehensive understanding of degradation mechanisms at HCDs, including corrosion, leaching, structural collapse, and bubble-induced stress, is lacking. Moreover, bridging the gap between the lab and industrial OER requires a standardized benchmark catalyst for HCD evaluation under industry-relevant conditions, including elevated temperatures (60–90 °C), high pressure (6–200 bar), and high alkaline electrolyte concentrations (20–30 wt%). Lastly, developing scalable and energy-efficient synthesis methods for the catalytic electrode is equally important for economic viability.

Conflicts of interest

There are no conflicts to declare.

Data availability

As this is a review article, no primary research results, data, software, or code have been included.

Acknowledgements

The authors would like to acknowledge the support from the CIPHER Project (IIID 2018-008) funded by the Commission on Higher Education – Philippine California Advanced Research Institutes (currently CHED–LAKAS Program). This research was also supported by the Korea Institute of Energy Technology Evaluation and Planning (KETEP) granted financial resources from the Ministry of Trade, Industry & Energy, Republic of Korea (20213030040590).

Notes and references

1 F. Zeng, C. Mebrahtu, L. Liao, A. K. Beine and R. Palkovits, *J. Energy Chem.*, 2022, **69**, 301–329.
2 Ö. N. Avcl, L. Sementa and A. Fortunelli, *ACS Catal.*, 2022, **12**, 9058–9073.
3 C. Kong, C. Zhi, Z. Wu, W. Yang, J. Yang and Z. Sun, *J. Colloid Interface Sci.*, 2024, **665**, 863–870.
4 C. Gort, P. W. Buchheister, M. Klingenhof, S. D. Paul, F. Dionigi, R. van de Krol, U. I. Kramm, W. Jaegermann, J. P. Hofmann, P. Strasser and B. Kaiser, *ChemCatChem*, 2023, **15**, e202201670.
5 M. R. Domalanta, J. N. Bamba, D. D. Matienzo, J. A. del Rosario-Paraggua and J. Ocon, *ChemSusChem*, 2023, **16**, e202300310.
6 P. Shi, X. Cheng and S. Lyu, *Chin. Chem. Lett.*, 2021, **32**, 1210–1214.
7 Y. Yao, J. Lyu, X. Li, C. Chen, F. Verpoort, J. Wang, Z. Pan and Z. Kou, *DeCarbon*, 2024, **5**, 100062.
8 Y. Zeng, M. Zhao, Z. Huang, W. Zhu, J. Zheng, Q. Jiang, Z. Wang and H. Liang, *Adv. Energy Mater.*, 2022, **12**, 2201713.
9 X. Luo, X. Tan, P. Ji, L. Chen, J. Yu and S. Mu, *EnergyChem*, 2023, **5**, 100091.
10 R. Chen, S. F. Hung, D. Zhou, J. Gao, C. Yang, H. Tao, H. Bin Yang, L. Zhang, L. Zhang, Q. Xiong, H. M. Chen and B. Liu, *Adv. Mater.*, 2019, **31**, 1903909.
11 T. Yang, J. Huang, Z. Liu and C. Chen, *Chem. Commun.*, 2025, **61**, 11681–11684.
12 E. Brim, K. K. Rücker, D. H. Taffa, D. W. Hayes, O. Bisen, S. Alia, M. Risch, J. Lorenz, C. Harms, M. Wark and R. M. Richards, *Chem. Commun.*, 2026, **62**, 763–774.
13 Y. Han, J. Wang, Y. Liu, T. Li, T. Wang, X. Li, X. Ye, G. Li, J. Li, W. Hu and Y. Deng, *Carbon Neutralization.*, 2024, **3**, 172–198.
14 A. Hao, Z. Liu and X. Ning, *J. Alloys Compd.*, 2024, **1003**, 175523.
15 M. Görlin, P. Chernev, P. Paciok, C. W. Tai, J. Ferreira de Araújo, T. Reier, M. Heggen, R. Dunin-Borkowski, P. Strasser and H. Dau, *Chem. Commun.*, 2019, **55**, 818–821.
16 S. Wang, A. Hao and Z. Liu, *ACS Appl. Nano Mater.*, 2024, **7**, 28602–28611.
17 Z. Cai, M. Xu, Y. Li, X. Zhou, K. Yin, L. Li, B. Jia, L. Guo and H. Zhao, *Carbon Energy*, 2024, **6**, e543.
18 J. Geppert, P. Röse, S. Czioska, D. Escalera-López, A. Boubnov, E. Saraçi, S. Cherevko, J. D. Grunwaldt and U. Krewer, *J. Am. Chem. Soc.*, 2022, **144**, 13205–13217.
19 M. Berger, I. M. Popa, L. Negahdar, S. Palkovits, B. Kaufmann, M. Pilaski, H. Hoster and R. Palkovits, *ChemElectroChem*, 2023, **10**, e202300235.
20 J. Qu, X. Hu, M. Deconinck, L. Liu, Y. Cheng, R. Zhao, M. Wang, H. Zhang, Y. Vaynzof, J. Schuster, A. Cabot, K. Leistner and F. Li, *ChemCatChem*, 2025, **17**, e202401667.
21 M. Nozari-Asbemarz, H. Imanzadeh, L. Hazraty, B. Babaei, A. Abbasi, S. S. Mehrabi-Kalajahi, M. A. Vafolomeev, J. J. Leahy and M. Amiri, *J. Power Sources*, 2025, **652**, 237555.
22 U. Shamraiz, B. Raza and A. Badshah, *Mater. Today Energy*, 2025, **53**, 102006.
23 Y. J. Son, K. Kawashima, R. A. Márquez, L. A. Smith, C. E. Chukwuneke and C. B. Mullins, *Curr. Opin. Electrochem.*, 2023, **39**, 101298.
24 Y. Pan, X. Xu, Y. Zhong, L. Ge, Y. Chen, J. P. M. Veder, D. Guan, R. O'Hayre, M. Li, G. Wang, H. Wang, W. Zhou and Z. Shao, *Nat. Commun.*, 2020, **11**, 2002.
25 F. Wu, F. Tian, M. Li, S. Geng, L. Qiu, L. He, L. Li, Z. Chen, Y. Yu, W. Yang and Y. Hou, *Angew. Chem., Int. Ed.*, 2025, **64**, e202413250.
26 Q. Xie, D. Ren, L. Bai, R. Ge, W. Zhou, L. Bai, W. Xie, J. Wang, M. Grätzel and J. Luo, *Chin. J. Catal.*, 2023, **44**, 127–138.
27 Z. Wang, W. A. Goddard and H. Xiao, *Nat. Commun.*, 2023, **14**, 4228.
28 M. Lu, Y. Zheng, Y. Hu, B. Huang, D. Ji, M. Sun, J. Li, Y. Peng, R. Si, P. Xi and C.-H. Yan, *Sci. Adv.*, 2022, **8**, eabq3563.
29 Z. Feng, P. Wang, Y. Cheng, Y. Mo, X. Luo, P. Liu, R. Guo and X. Liu, *J. Electroanal. Chem.*, 2023, **946**, 117703.
30 L. Wei, D. Meng, Q. Jiang, W. Wang and J. Tang, *J. Environ. Chem. Eng.*, 2022, **10**, 108591.
31 S. Iqbal, J. C. Ehlers, I. Hussain, K. Zhang and C. Chatzichristodoulou, *Chem. Eng. J.*, 2024, **499**, 156219.
32 M. Gong and H. Dai, *Nano Res.*, 2015, **8**, 23–39.
33 J. Zhang, J. R. Winkler, H. B. Gray and B. M. Hunter, *Energy and Fuels*, 2021, **35**, 19164–19169.
34 D. Friebel, M. W. Louie, M. Bajdich, K. E. Sanwald, Y. Cai, A. M. Wise, M. J. Cheng, D. Sokaras, T. C. Weng, R. Alonso-Mori, R. C. Davis, J. R. Bargar, J. K. Nørskov, A. Nilsson and A. T. Bell, *J. Am. Chem. Soc.*, 2015, **137**, 1305–1313.
35 S. Anantharaj, S. Kundu and S. Noda, *Nano Energy*, 2021, **80**, 105514.
36 S. Khatun, S. Pal and P. Roy, *J. Alloys Compd.*, 2024, **977**, 173393.
37 X. Wang, Z. Jiang, Y. Ma, X. Su, X. Zhao, A. Zhu and Q. Zhang, *J. Power Sources*, 2024, **591**, 233819.
38 E. Lee, A. H. Park, H. U. Park and Y. U. Kwon, *Ultrason. Sonochem.*, 2018, **40**, 552–557.
39 M. Gorlin, J. F. De Araujo, H. Schmies, D. Bernsmeier, S. Dresp, M. Gliech, Z. Jusys, P. Chernev, R. Kraehnert, H. Dau and P. Strasser, *J. Am. Chem. Soc.*, 2017, **139**, 2070–2082.
40 S. Zhang, S. Huang, F. Sun, Y. Li, L. Ren, H. Xu, Z. Li, Y. Liu, W. Li, L. Chong and J. Zou, *J. Energy Chem.*, 2024, **88**, 194–201.
41 C. Liang, P. Zou, A. Nairan, Y. Zhang, J. Liu, K. Liu, S. Hu, F. Kang, H. J. Fan and C. Yang, *Energy Environ. Sci.*, 2020, **13**, 86–95.
42 Y. Wu, H. Wang, S. Ji, X. Tian, G. Li, X. Wang and R. Wang, *Appl. Surf. Sci.*, 2021, **564**, 150440.
43 G. Zhang, J. Zeng, J. Yin, C. Zuo, P. Wen, H. Chen and Y. Qiu, *Appl. Catal., B*, 2021, **286**, 119902.
44 S. Kang, C. Im, I. Spanos, K. Ham, A. Lim, T. Jacob, R. Schlögl and J. Lee, *Angew. Chem., Int. Ed.*, 2022, **61**, e202214541.
45 M. Yan, Z. Zhao, P. Cui, K. Mao, C. Chen, X. Wang, Q. Wu, H. Yang, L. Yang and Z. Hu, *Nano Res.*, 2021, **14**, 4220–4226.
46 Y. Zhang, L. Liu, J. Wang, R. Yao, Y. Wu, M. Wang, Q. Zhao, J. Li and G. Liu, *J. Power Sources*, 2022, **518**, 230757.
47 L. Fan, Q. Geng, L. Ma, C. Wang, J. X. Li, W. Zhu, R. Shao, W. Li, X. Feng, Y. Yamauchi, C. Li and L. Jiang, *Chem. Sci.*, 2023, **14**, 13851–13859.
48 Q. Geng, L. Fan, H. Chen, C. Zhang, Z. Xu, Y. Tian, C. Yu, L. Kang, Y. Yamauchi, C. Li and L. Jiang, *J. Am. Chem. Soc.*, 2024, **146**, 10599–10607.
49 Y. Li, R. Tong, W. Zhang and S. Peng, *J. Catal.*, 2022, **410**, 22–30.
50 Y. Sheng, M. Manuputty, M. Kraft and R. Xu, *ACS Appl. Energy Mater.*, 2023, **6**, 2320–2332.
51 J. Hu, J. Yin, A. Peng, D. Zeng, J. Ke, J. Liu and K. Guo, *Small*, 2024, **20**, 2402881.
52 L. He, N. Wang, M. Xiang, L. Zhong, S. Komarneni and W. Hu, *Appl. Catal., B*, 2024, **345**, 123686.
53 Y. Zhao, W. Wan, N. Dongfang, C. A. Triana, L. Douls, C. Huang, R. Erni, M. Iannuzzi and G. R. Patzke, *ACS Nano*, 2022, **16**, 15318–15327.
54 P. Zhai, C. Wang, Y. Zhao, Y. Zhang, J. Gao, L. Sun and J. Hou, *Nat. Commun.*, 2023, **14**, 1873.
55 M. Batool, A. Hameed and M. A. Nadeem, *Coord. Chem. Rev.*, 2023, **480**, 215029.

56 H. W. Choi, D. I. Jeong, S. Bin Kwon, S. Woo, J. Kim, J. H. Kim, W. S. Yang, B. Lim, B. K. Kang and D. H. Yoon, *Appl. Surf. Sci.*, 2021, **566**, 150706.
57 X. Wu, X. Gu, J. Tai, J. Tang, K. Yuan, L. Liu, Y. Zheng, A. Altaf, X. Shen and S. Cui, *J. Power Sources*, 2025, **633**, 236430.
58 Y. Li, H. Guo, J. Zhao, Y. Zhang, L. Zhao and R. Song, *Chem. Eng. J.*, 2023, **464**, 142604.
59 Y. Wang, W. Nong, N. Gong, T. Salim, M. Luo, T. L. Tan, K. Hippalgaonkar, Z. Liu and Y. Huang, *Small*, 2022, **18**, 2203340.
60 X. Liu, X. Fan, H. Huang, H. Lin and J. Gao, *J. Colloid Interface Sci.*, 2021, **587**, 385–392.
61 Y. Wu, Y. Li, Z. Xie, Y. Wang, Y. Wang and B. Wei, *Chem. Eng. J.*, 2024, **488**, 151086.
62 X. Wan, Y. Song, H. Zhou and M. Shao, *Energy Mater. Adv.*, 2022, **2022**, 9842610.
63 J. Yu, D. Huang, L. Zhou, W. Liu and D. Zhou, *J. Power Sources*, 2025, **647**, 237341.
64 S. Assavachin, S. Ittisanronnachai, T. Atithep, N. Chitterisin and M. Sawangphruk, *J. Power Sources*, 2025, **650**, 237494.
65 J. Mohammed-Ibrahim, *J. Power Sources*, 2020, **448**, 227375.
66 Y. H. Wang, L. Li, J. Shi, M. Y. Xie, J. Nie, G. F. Huang, B. Li, W. Hu, A. Pan and W. Q. Huang, *Adv. Sci.*, 2023, **10**, 2303321.
67 H. Wang and S. Chen, *Catalysts*, 2024, **14**, 81.
68 C. Feng, F. Wang, Z. Liu, M. Nakabayashi, Y. Xiao, Q. Zeng, J. Fu, Q. Wu, C. Cui, Y. Han, N. Shibata, K. Domen, I. D. Sharp and Y. Li, *Nat. Commun.*, 2021, **12**, 5980.
69 Y. Qiu, Z. Liu, A. Sun, X. Zhang, X. Ji and J. Liu, *ACS Sustainable Chem. Eng.*, 2022, **10**, 16417–16426.
70 J. Xing, S. Bliznakov, L. Bonville, R. Maric and A. Friedman, *ChemCatChem*, 2025, **17**, e202402165.
71 H. Qiu, K. Obata, K. Tsuburaya, T. Nishimoto, K. Nagato and K. Takanabe, *J. Power Sources*, 2024, **611**, 234765.
72 D. Senthil Raja, C. L. Huang, Y. A. Chen, Y. M. Choi and S. Y. Lu, *Appl. Catal., B*, 2020, **279**, 119375.
73 X. Wang, Z. Qin, J. Qian, L. Chen and K. Shen, *Appl. Catal., B*, 2024, **359**, 124506.
74 X. Dong, E. Yan, Y. Lv, Y. Zhou and X. Chu, *Appl. Catal., A*, 2024, **681**, 119772.
75 C. Dang Van, S. Kim, M. Kim and M. H. Lee, *ACS Sustainable Chem. Eng.*, 2023, **11**, 1333–1343.
76 X. Liu, S. Jing, C. Ban, K. Wang, Y. Feng, C. Wang, J. Ding, B. Zhang, K. Zhou, L. Gan and X. Zhou, *Nano Energy*, 2022, **98**, 107328.
77 Y. Huang, T. Zhou, Y. Hu, Y. Yang, F. Yang, W. Huang, L. He and W. Sun, *Int. J. Hydrogen Energy*, 2023, **48**, 33411–33421.
78 B. Wang, H. Sun, M. Chen, T. Zhou, H. Zheng, M. Zhang, B. Xiao, J. Zhao, Y. Zhang, J. Zhang and Q. Liu, *Chem. Eng. J.*, 2024, **479**, 147500.
79 Y. Hu, T. Shen, Z. Song, Z. Wu, S. Bai, G. Liu, X. Sun, Y. Wang, S. Hu, L. Zheng and Y. F. Song, *ACS Catal.*, 2023, **13**, 11195–11203.
80 F. Jiang, Y. Li and Y. Pan, *Adv. Mater.*, 2024, **36**, 2306309.
81 Y. Zhu, Z. Li and Y. Zhou, *ChemCatChem*, 2025, e202500072.
82 N. Yang, H. Li, X. Lin, S. Georgiadou, L. Hong, Z. Wang, F. He, Z. Qi and W. F. Lin, *J. Energy Chem.*, 2025, **105**, 669–701.
83 J. N. Bamba, A. T. Dumlao, R. M. Lazaro, D. D. Matienzo and J. Ocon, *Curr. Opin. Electrochem.*, 2024, **48**, 101592.
84 Y. Li, X. Lin, Y. Yang, S. Georgiadou, B. Du, Z. Qi, S. Saremi-Yarahmadi and W. F. Lin, *ChemCatChem*, 2025, **17**, e01040.
85 P. Liu, J. Wang, X. Wang, L. Liu, X. Yan, H. Wang, Q. Lu, F. Wang and Z. Ren, *Int. J. Hydrogen Energy*, 2024, **49**, 285–294.
86 Q. N. Ha, C. H. Yeh, N. S. Gultom and D. H. Kuo, *J. Mater. Chem. A*, 2023, **12**, 460–474.
87 S. Kang, D. Yeol Lee, Y. Kim, S. Bae and J. Lee, *Chem. Eng. J.*, 2024, **499**, 156469.
88 Y. Son, J. Mo, E. Yong, J. Ahn, G. Kim, W. Lee, C. H. Kwon, H. Ju, S. W. Lee, B. H. Kim, M. Kim and J. Cho, *Appl. Catal., B*, 2024, **343**, 123563.
89 Y. Zhao, Q. Wen, D. Huang, C. Jiao, Y. Liu, Y. Liu, J. Fang, M. Sun and L. Yu, *Adv. Energy Mater.*, 2023, **13**, 2203595.
90 N. Zhou, R. Liu, X. Wu, Y. Ding, X. Zhang, S. Liang, C. Deng, G. Qin, Z. Huang and B. Chen, *J. Power Sources*, 2023, **574**, 233163.
91 R. Kaur, A. Gaur, V. Pundir, K. Arun and V. Bagchi, *J. Colloid Interface Sci.*, 2024, **672**, 736–743.
92 J. Liu, G. Qian, T. Yu, J. Chen, C. Zhu, Y. Li, J. He, L. Luo and S. Yin, *Chem. Eng. J.*, 2022, **431**, 134247.
93 P. Tan, Y. Wu, Y. Tan, Y. Xiang, L. Zhou, N. Han, Y. Jiang, S. J. Bao and X. Zhang, *Small*, 2024, **20**, 2308371.
94 Y. Y. Feng, G. Deng, X. Y. Wang, M. Zhu, Q. N. Bian and B. S. Guo, *Int. J. Hydrogen Energy*, 2023, **48**, 12354–12363.
95 Y. F. Song, Z. Y. Zhang, H. Tian, L. Bian, Y. Bai and Z. L. Wang, *Chem. – Eur. J.*, 2023, **29**, e202301124.
96 M. Liu, J. Wang, H. Wu, S. Li, Y. Shi and N. Cai, *Int. J. Hydrogen Energy*, 2024, **51**, 626–637.